Electron Injection through a Specific Pathway Determines the Outcome of Oxygen Activation at the Diiron Cluster in the F208Y Mutant of *Escherichia coli* Ribonucleotide Reductase Protein R2†

Sara E. Parkin,‡ Shuxian Chen,§ Brenda A. Ley,‡ Lara Mangravite,‡ Dale E. Edmondson,|| Boi Hanh Huynh,§ and J. Martin Bollinger, Jr.*,‡

Department of Biochemistry and Molecular Biology, The Pennsylvania State University, University Park, Pennsylvania 16802, and Departments of Physics, Chemistry, and Biochemistry, Emory University, Atlanta, Georgia 30322

Received September 24, 1997

ABSTRACT: Protein R2 of ribonucleotide reductase from *Escherichia coli* contains a dinuclear iron cluster, which reductively activates O_2 to produce the enzyme's functionally essential tyrosyl radical by one-electron oxidation of residue Y122. A key step in this reaction is the rapid injection of a single electron from an exogenous reductant (Fe^{2+} or ascorbate) during formation of the radical-generating intermediate, cluster X, from the diiron(II) cluster and O_2. As this step leaves only one of the two oxidizing equivalents of the initial diiron(II)−O_2 adduct, it commits the reaction to a one-electron oxidation outcome and precludes possible two-electron alternatives (as occur in the related diiron bacterial alkane hydroxylases and fatty acyl desaturases). In the F208Y site-directed mutant of R2, Y208 is hydroxylated (a two-electron oxidation) in preference to the normal reaction [Åberg, A., Ormö, M., Nordlund, P., & Sjöberg, B. M. (1993) *Biochemistry 32,* 9845−9850], implying that this substitution blocks electron injection or (more likely) introduces an endogenous reductant (Y208) that effectively competes. Here we demonstrate that O_2 activation in the F208Y mutant of R2 partitions between these two-electron (Y208 hydroxylation) and one-electron (Y122 radical production) outcomes and that the latter becomes predominant under conditions which favor electron injection (namely, high concentration of the reductant ascorbate). Moreover, we show that the sensitivity of the partition ratio to ascorbate concentration is strictly dependent on the integrity of a hydrogen-bond network involving the near surface residue W48: when this residue is substituted with F, Y208 hydroxylation predominates irrespective of ascorbate concentration. These data suggest that the hydrogen-bond network involving W48 is a specific electron-transfer pathway between the cofactor site and the protein surface.

The R2 subunits of the ribonucleotide reductases (RNRs[1]) from mammals, several medically important viruses (e.g., herpes simplex), and aerobically growing *Escherichia coli* belong to a class of proteins that use carboxylate-bridged diiron(II) clusters to reductively activate molecular oxygen for difficult oxidation reactions (see refs *1* and *2* for recent reviews). Other members of this class include plant fatty acyl desaturases, such as stearoyl acyl carrier protein Δ-9 desaturase (*3*−*5*), and bacterial hydrocarbon hydroxylases, such as methane monooxygenase (*6*−*10*), toluene-4-monooxygenase (*11*), and alkane ω-hydroxylase (*12*). While these enzymes share a common functional motif [reaction of O_2 at a diiron(II) cluster], the outcomes of their reactions are chemically distinct: O_2 activation in R2 results in one-electron oxidation of an endogenous tyrosine residue [generating the stable tyrosyl radical that is required for RNR catalytic activity (*13, 14*)], whereas the bacterial alkane hydroxylases and fatty acyl desaturases catalyze distinct two-electron oxidation reactions—hydroxylation and dehydrogenation (respectively) of unactivated hydrocarbon substituents (*15, 16*). A unifying objective of research on the diiron proteins is to understand the relationship between the structure of each protein and its diiron cofactor and the mechanism and outcome of its O_2 reaction. Protein R2 from *E. coli* presents a unique opportunity to define such structure−function relationships. The three-dimensional structures of its (reactant) diiron(II) and (product) diiron(III) forms have been solved to high resolution (*17, 18*), it has been expressed to high levels in *E. coli* (*19, 20*) and can be manipulated by mutagenesis (*21*), and most importantly, the outcome of its O_2 reaction can be altered: in the site-directed mutant R2 in which residue F208 is replaced with Y, the Y208 residue undergoes *o*-hydroxylation in preference to the normal one-electron oxidation of Y122 (*22*). The

† This work was supported by NIH Grants GM55365 (J.M.B.) and GM47295 (B.H.H. and D.E.E.) and by a grant from The Searle Scholars Program of The Chicago Community Trust (J.M.B.). L.M. was supported as a Pfizer Undergraduate Summer Research Fellow.

* To whom correspondence should be addressed: Tel (814) 863-5707; Fax (814) 863-7024; E-mail jmb21@psu.edu.

‡ Department of Biochemistry and Molecular Biology, Penn State University.

§ Department of Physics, Emory University.

|| Departments of Chemistry and Biochemistry, Emory University.

[1] Abbreviations: RNR, ribonucleotide reductase; EPR, electron paramagnetic resonance; IPTG, isopropyl thiogalactopyranoside; PCR, polymerase chain reaction; LB, Luria−Bertani; PMSF, phenylmethanesulfonyl fluoride; equiv, equivalents; UV, ultraviolet.

S0006-2960(97)02371-4 CCC: $15.00
Published on Web 01/08/1998

Scheme 1

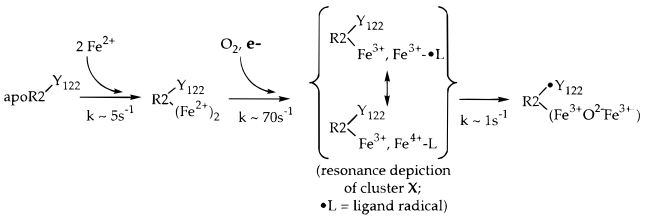

Scheme 2

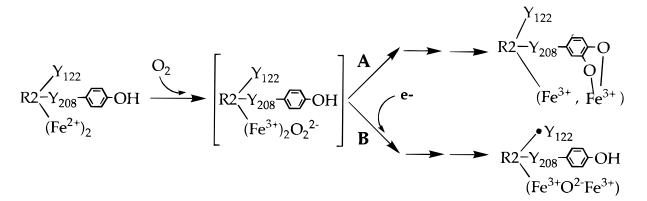

Y208-derived catechol then becomes a bidentate ligand to one Fe(III) ion of the cluster. The resulting complex [hereafter referred to as a diiron(III)−catecholate] exhibits an intense absorption band centered near 675 nm which acts as a "reporter" for the altered reaction (*23*). A detailed understanding of the mechanisms of the wild-type R2 reaction and the R2-F208Y hydroxylation reaction might provide significant insight into mechanism and outcome determinants for O_2 activation by the diiron proteins.

Past investigations of the wild-type R2 reaction have established that it proceeds according to the sequence shown in Scheme 1 when carried out at 5 °C with excess Fe^{2+} or in the presence of the reductant ascorbate (*24*−*27*). A key step in this mechanism is the rapid injection of an electron (e^- in Scheme 1) from Fe^{2+} or ascorbate during formation of the radical-generating intermediate, cluster X, from the diiron(II) cluster and O_2 (*27*). This step may serve to prevent accumulation of two-electron oxidized intermediates [such as the (formally) diiron(IV) cluster Q that accumulates during O_2 activation by methane monooxygenase (*28*−*30*)] and thereby to preclude possible two-electron alternatives to tyrosyl radical production. Mediating electron injection may thus be a means by which the R2 protein directs the outcome of its O_2 reaction. The fact that a two-electron oxidation *does* occur in the F208Y mutant (*22*, *23*) implies that electron injection is subverted in this mutant. Most likely, Y208 competes effectively with electron injection for reduction of an early, two-electron-oxidized intermediate.

Scheme 2 illustrates the hypothesis that the O_2 reaction of R2-F208Y might partition between hydroxylation of Y208 (top branch) and the normal outcome, one-electron oxidation of Y122 (bottom branch). Indeed, a weak, sharp 410 nm absorption (characteristic of tyrosyl radical) was observed upon reaction of apo R2-F208Y with Fe^{2+} and O_2 (*22*), and EPR analysis indicated the formation of 0.18 equiv of tyrosyl radical relative to R2 homodimer (*31*). This metastable radical ($t_{1/2}$ of 10 min at 25 °C) was assigned to Y122 (as opposed to Y208) on the basis of its EPR line shape and relaxation properties (*31*).[2] In the mechanism of Scheme 2, the partition ratio would depend upon the relative rates of electron injection (step B) versus the unimolecular step that commits the reaction to Y208 hydroxylation (step A). The formation of detectable quantities of Y122 radical would imply that the rates of the bifurcating steps are similar. Therefore, we considered that it might be possible to alter the product distribution (partition ratio) either by changing reaction conditions to favor electron injection or by mutagenizing the protein to disfavor this step. Herein we demonstrate that formation of the diiron(III)−catecholate is indeed suppressed and production of the Y122 radical and normal μ-oxo-diiron(III) cluster enhanced by the presence of high concentrations of the reductant ascorbate. Conversely, we show that substitution (with phenylalanine) of tryptophan residue 48 (W48), which is part of a surface-to-diiron cluster hydrogen-bond network (*17*) that we and others have proposed mediates electron transfer into the diiron-radical site of R2 (*17*, *32*−*34*), completely suppresses formation of Y122 radical and drastically reduces production of the μ-oxo-diiron(III) cluster in favor of the diiron(III)−catecholate. Most importantly, we demonstrate that the W48F mutation completely eliminates the effect of ascorbate on the partition ratio. These data provide evidence that W48 is essential for electron injection into the reacting diiron site of R2-F208Y and lend credence to our earlier proposal that this pathway mediates rapid electron injection during the exclusively one-electron oxidation chemistry of the wild-type protein (*32*).

MATERIALS AND METHODS

Materials. *E. coli* strain N6405 containing the plasmid pSPS2 (*19*) and oligonucleotide primers for DNA sequencing were generously provided by Professor J. Stubbe. Culture medium components were purchased from Marcor Development Corp. (Hackensack, NJ). Isopropyl thiogalactopyranoside (IPTG) was purchased from Biosynth International (Naperville, IL). Ampicillin and 1,10-phenanthroline were purchased from Sigma. Oligonucleotides were purchased from the Nucleic Acid Facility of the Penn State University Biotechnology Institute. Reagents for the polymerase chain reaction were purchased from New England Biolabs (Beverly, MA). Restriction enzymes and other DNA modifying enzymes were purchased from New England Biolabs, Boehringer Mannheim (Indianapolis, IN), and Promega (Madison, WI).

Preparation of Expression Vectors for Mutant R2 Proteins. The F208Y and W48F mutations[3] were introduced separately into the *nrdB* gene (encoding R2) by using the polymerase chain reaction (PCR). In preparation of *nrdB-F208Y*, the gene was amplified in two fragments by using four primers and a single colony of *E. coli* strain N6405/pSPS2 in each reaction as template. The 5′-most 648 base pairs were amplified with primers 1 (5′- CAG GAC ACA **CAT ATG** GCA TAT ACC ACC -3′) and 2 (5′- GGA ACA AGC A**AA GCT T**AC GTA GTA ACG AAT CGC -3′). Primer 1 introduced an *Nde*I restriction site (in boldface type) incorporating the start codon of *nrdB* to allow for ligation

[2] The EPR line shapes of tyrosyl radicals are largely determined by the magnitudes of the β-proton hyperfine couplings, which are extremely sensitive to the angle between the phenol ring and the β-C−H bonds (*41*, *42*). Thus, EPR line shape is diagnostic of the conformation of the Y radical. Moreover, the Y122 radical in R2 interacts weakly with the diiron center, and this interaction enhances electronic relaxation (*43*, *44*), rendering this property also somewhat diagnostic of its environment.

[3] The posttranslationally cleaved intiator Met is designated residue zero and the nucleotide triplet encoding it as codon zero.

directly into the pET-22b expression vector (Novagen). Primer 2 introduced the desired mutation at codon F208 (TTC to TAC, complement of underlined triplet) and a silent mutation (GTC to GTA) in codon V210 (mutation italicized), which produced a unique *Hin*dIII site (in boldface type) for internal ligation of the two *nrdB* fragments. The 3′-most 510 base pairs of the gene were amplified by using primers 3 (5′ -CGT TTC TAC GT**A AGC TT**T GCT TGT TCC -3′) and 4 (5′- GTG TG**C TCG AG**A TGC GCA GGG TAA CG -3′). Primer 3 introduced the aforementioned silent mutation at codon V210 (italicized) to create the unique *Hin*dIII site (in boldface type) for internal ligation, while primer 4 introduced an *Xho*I site (in boldface type) 3′ of *nrdB* for ligation into pET22b. The 5′ PCR fragment was digested with *Nde*I and *Hin*dIII, the 3′ PCR fragment with *Hin*dIII and *Xho*I, and the vector pET22b with *Nde*I and *Xho*I. The fragments were joined in a three-piece ligation reaction to give the expression vector pR2-F208Y. The sequence of the coding region of this plasmid was verified to ensure that no unwanted mutations had been introduced during amplification.

The W48F mutation was introduced via PCR by making use of the unique *Aat*II restriction site in codon V55 of *nrdB*. The 220 base pairs of pR2-F208Y immediately 5′ of *nrdB* and the first 172 base pairs of the gene were amplified (single fragment) by using primers 5 (5′- GAA GTG GCG AGC CCG ATC TTC CCC -3′) and 6 (5′- GGG A**GA CGT C**AA C*C*T C*C*T CCG GAC GAA AGA AGA AAG AGA GC-3′) and purified pR2-F208Y as template. Primer 5 was designed to anneal ∼110 base pairs 5′ of a unique *Bgl*II site, which is 105 base pairs 5′ of the start of *nrdB* in pR2-F208Y. Primer 6 was designed to anneal 3′ of codon 55, span the unique *Aat*II restriction site (in boldface type), and introduce the desired mutation at codon 48 (TGG to TTT, complement of underlined triplet). Primer 6 also introduced silent (GAA to GAG) mutations in codons 51 and 52 (mutations italicized) to circumvent potential primer hairpin formation due to self-complementarity in this portion of the *nrdB* sequence. The 392 base pair PCR fragment and the vector pR2-F208Y were both digested with *Bgl*II and *Aat*II, and the remaining 270 base pair fragment of the original PCR product was ligated with the vector to give pR2-W48F/F208Y. The entire *nrdB* coding sequence was again verified.

Hyperexpression and Purification of Mutant R2 Proteins. E. coli strain BL21(DE3) (Novagen) transformed with pR2-F208Y or pR2-W48F/F208Y was grown with vigorous aeration at 37 °C in LB medium supplemented with 150 μg/mL ampicillin. When the culture reached OD_{600} of 0.7−0.9, 1,10-phenanthroline (100 mM dissolved in 100 mM HCl) was added to a final concentration of 100 μM. The culture was incubated an additional 15 min, and then expression of the R2 mutant protein was induced by addition of IPTG to a concentration of 200 μM. The culture was grown an additional 3−4 h, cooled to ∼15 °C, and harvested by centrifugation. Pelleted cell mass was frozen in liquid N_2 and stored at −80 °C until use. A typical yield was 2.5 g of wet cell paste/L of culture.

The mutant R2 proteins were purified at 4 °C by a procedure similar to that previously used for wild-type R2 (*19*, *26*). In a typical purification, 100 g of frozen cell paste was thawed and resuspended in 500 mL of buffer A [50 mM Tris-HCl, pH 7.6, and 5%(w/v) glycerol] containing 0.25 mM phenylmethanesulfonyl fluoride (PMSF) and 1 mM 1,10-phenanthroline. Cell lysis, streptomycin sulfate precipitation, and ammonium sulfate precipitation steps were carried out as previously described, except that *neither ferrous ammonium sulfate nor sodium ascorbate was added* to the crude cell lysate. The pellet from the ammonium sulfate step was redissolved in 90 mL of buffer A containing 0.25 mM PMSF and 1 mM 1,10-phenanthroline, and this solution was dialyzed for 4 h against 6 L of buffer A. An equal volume of buffer A containing 0.25 mM PMSF was added to the dialysate, and the solution was loaded on a 7.5 cm × 47 cm (2 L) DEAE Bio-Gel A (Bio-Rad) column equilibrated in buffer A. The column was washed with 1.8 L of buffer A followed by 2 L of buffer A containing 105 mM NaCl. The R2 protein was then eluted with buffer A containing 140 mM NaCl. Fractions containing protein (as judged by their light absorption spectra) were pooled, the pool (∼1 L) was diluted with an equal volume of buffer A containing 0.25 mm PMSF, and this solution was loaded on a 5 cm × 55 cm Q-Sepharose Fast Flow (Pharmacia) column equilibrated in buffer A. The column was washed with 0.6 L of buffer A, followed by 1.5 L of buffer A containing 225 mM NaCl. The protein was then eluted with buffer A containing 300 mm NaCl. Fractions containing the protein were pooled (∼0.5 L), and the pool was concentrated 20-fold by ultrafiltration (in an Amicon cell equipped with a YM30 membrane). The protein was dialyzed to equilibrium against 100 mM Na-Hepes buffer, pH 7.6 (buffer B), flash-frozen in liquid N_2, and stored at −80 °C. Denaturing polyacrylamide gel electrophoresis revealed the protein to be > 95% pure. A typical yield was 3 g.

Determination of Protein Concentration. Concentrations of R2 mutant apoproteins were determined spectrophotometrically by using molar absorption coefficients at 280 nm (ϵ_{280}) calculated by the method of Gill and von Hippel (*35*). It was found that the value for wild-type apo-R2 calculated by this method (120 mM^{-1} cm^{-1}) agrees with the experimentally determined value [120 mM^{-1} cm^{-1} (*36*)], validating the values calculated for the mutant apoproteins (ϵ_{280} = 122 mM^{-1} cm^{-1} for apo-R2-F208Y and 111 mM^{-1} cm^{-1} for apo-R2-W48F/F208Y).

Reaction of R2 Mutants with Fe^{2+} and O_2. Samples of apo-R2-F208Y or apo-R2-W48F/F208Y (∼0.30 mM) in buffer B were rendered anoxic on a vacuum line by multiple cycles of gentle evacuation and refilling with argon (purified through an Oxisorb-Glas cartridge from MG Industries). After ∼5 such cycles the protein was allowed to reach equilibrium with the vapor phase by 1 h of gentle stirring on ice. Two additional evacuation−refill−equilibration cycles were carried out, the vessel containing the protein was sealed by closing the stopcock, and the protein was taken into a glovebox (MBraun) maintained at <1 ppm O_2. Multiple 0.2 mL aliquots of the protein were adjusted to different concentrations of ascorbate by addition of either 2 M sodium ascorbate in buffer B, buffer B lacking ascorbate, or a combination of the two. After gentle mixing, an aliquot of an anoxic solution of $^{56}Fe^{2+}$ (10 mM) or $^{57}Fe^{2+}$ (20 mM) was added to each aliquot of apo-R2 so as to deliver 3 equiv of Fe^{2+} relative to apo-R2 dimer. The Fe^{2+}−R2 solutions (with varying concentrations of ascorbate) were sealed in microcentrifuge tubes with rubber septa, removed from the anoxic chamber, and incubated on ice. After sufficient time

for temperature equilibrium to be reached (>10 min), an equal volume of ice-cold, O_2-saturated buffer B was injected forcefully via a gastight syringe while the sample was gently vortexed. In experiments to monitor tyrosyl radical produced, the UV−visible light absorption spectrum of each sample was recorded on an HP8453 diode array spectrometer (Hewlett-Packard) immediately after introduction of the O_2-saturated buffer. Identical samples prepared in parallel were quickly transferred to EPR tubes and frozen by immersion in liquid N_2-chilled 2-methylbutane. In experiments to characterize only the Fe products of the reaction, the samples were incubated at ambient temperature long enough (1 h) to allow tyrosyl radical to decay, and UV−visible light absorption spectra were then recorded. In preparation of Mössbauer samples, four or five identical samples (prepared as above) were combined and concentrated ~5-fold in a Centricon 30 microconcentrator (Amicon). This sample was then transferred to a Mössbauer cell and frozen in liquid N_2 for later analysis.

EPR Spectroscopy. EPR spectra at X-band were recorded on a Bruker ESP 300 spectrometer maintained at 100 K by a Bruker ER4111VT cryostat system. Spectral parameters are given in the figure legends. Concentrations of tyrosyl radical were determined by double integration and comparison to a Cu^{2+}−perchlorate standard (*37*). Double integrals of sample and standards were corrected for differences in *g*-value as previously described (*38*).

Mössbauer Spectroscopy. Mössbauer spectra were recorded at 4.2 K with a magnetic field of 0.05 T applied parallel to the incident γ-beam. The spectrometer has been described (*39*).

RESULTS AND DISCUSSION

Preparation of Unmodified Apo-R2-F208Y and Apo-R2-W48F/F208Y. The hydroxylation of Y208 that occurs in the R2-F208Y mutant protein (*22, 23*) is an irreversible, stoichiometric (as opposed to catalytic) reaction. Therefore, investigation of the reaction in vitro requires a method for isolating the protein in its unmodified form, which requires preventing its exposure to Fe^{2+} or O_2 (or both) during expression and purification. We judged that the published procedure (*22*) would not be cost-effective for obtaining the gram quantities of protein needed for our studies, and therefore, we developed an alternative method. The simple strategy of chelating available Fe^{2+} by addition of the cell-permeative 1,10-phenanthroline shortly before induction of protein expression[4] and again during early steps of purification proved effective. The R2 mutant proteins prepared in this manner have <0.2 Fe/R2 dimer (as determined by a published colorimetric assay) and take up 3.0−3.2 Fe^{2+}/R2 dimer during "reconstitution" (as determined by spectrophotometrically monitored aerobic titration of the protein with Fe^{2+} and subsequent analysis of stably bound Fe; data not shown). These values are comparable to those determined for the wild-type protein isolated by the traditional method (*26, 40*), which involves a postpurification, denaturing chelation step (*13*).[5] Moreover, this procedure is quite amenable to large-scale fermentations, and we have used it to obtain multigram quantities of the unmodified forms of these and other R2 mutant apoproteins.

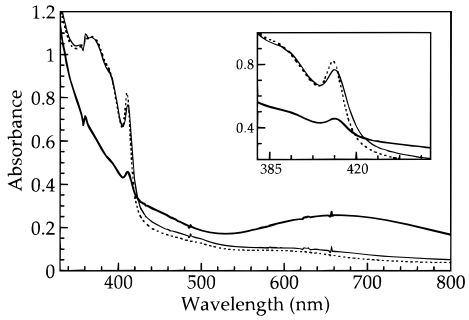

FIGURE 1: UV−visible light absorption spectra produced upon reaction at 5 ± 3 °C of Fe^{2+}−R2-F208Y (0.10 mM protein, Fe^{2+}/R2 = 3) with excess O_2 (~650 μM) in the absence of reductant (thicker solid line) and in the presence of 106 mM sodium ascorbate (thinner solid line). The dashed line is a reference spectrum of wild-type R2 reacted in the absence of ascorbate under identical conditions, with the exception that the Fe^{2+}/R2 ratio was 4 (to ensure that Fe^{2+} was in excess). The inset is a "blow-up" of the sharp 410 nm feature of the tyrosyl radical. Details of sample preparation are given in Materials and Methods.

Effect of Varying Ascorbate Concentration on Products of O_2 Reaction of R2-F208Y. In agreement with the work of Åberg et al. (*22*), reaction of the Fe^{2+} complex of R2-F208Y with O_2 results in the development of an absorption spectrum that is very different from that of wild-type R2 and that is characterized by a broad absorption band centered at ~675 nm (Figure 1, thicker solid line). It was previously inferred by comparison of this spectrum to those of model complexes, and subsequently confirmed by X-ray crystallographic analysis of R2-F208Y, that this feature arises from hydroxylation of Y208 and chelation of one of the Fe(III) ions of the cluster by the resulting catechol (*23*). In addition to this altered product, a significant quantity of tyrosyl radical is also produced (*22*), as reflected by the sharp absorption peak at 410 nm and the characteristic EPR doublet (Figure 2, spectrum A). Spin quantitation from this EPR spectrum gave 0.25 ± 0.04 equiv of tyrosyl radical, in agreement with previous reports (*22, 31*). The Mössbauer spectrum of a sample prepared identically (Figure 3, spectrum A) is dominated by a central doublet (82% ± 4% of the total iron absorption), which can be analyzed either as a single quadrupole doublet with the Mössbauer parameters shown in Table 1 or as two unresolved quadrupole doublets with only slightly different parameters and somewhat reduced line widths. As the additional complexity of the latter analysis is not justified by a significant improvement in agreement with the experimental spectrum, only the former is shown in Figure 3A (dashed line plotted above the experimental spectrum). We assign this apparent doublet to the two (unresolved) sites of the diiron(III)−catecholate product, on the following basis: (1) it is the primary product, and X-ray crystallographic analysis of R2-F208Y implies that the diiron(III)−catecholate is the primary product (*22*); (2) these parameters are typical for high-spin Fe(III) ions, and the much reduced ΔE_Q value relative to the two sites of the μ-oxo-diiron(III) cluster is consistent with the absence of a

[4] Note that the concentration of phenanthroline needed to reduce available Fe^{2+} to acceptable levels is dependent on the composition of the growth medium and must be empirically determined.

[5] It remains unclear why R2 proteins isolated to date in different laboratories by different methods (*20, 40, 45*) bind less than the theoretical complement of Fe (4 Fe/R2 dimer).

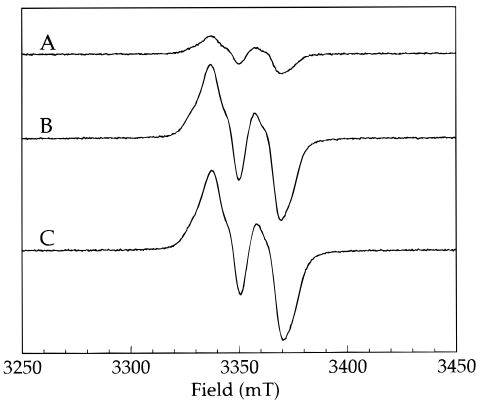

FIGURE 2: Electron paramagnetic resonance spectra at 100 K of R2-F208Y reacted as described in the legend to Figure 1 (A) in the absence of ascorbate and (B) in the presence of 106 mM sodium ascorbate. Spectrum C is of the wild-type R2 reference sample described in the legend to Figure 1. The spectra were acquired with a microwave power of 0.2 mW and a modulation amplitude of 4 G.

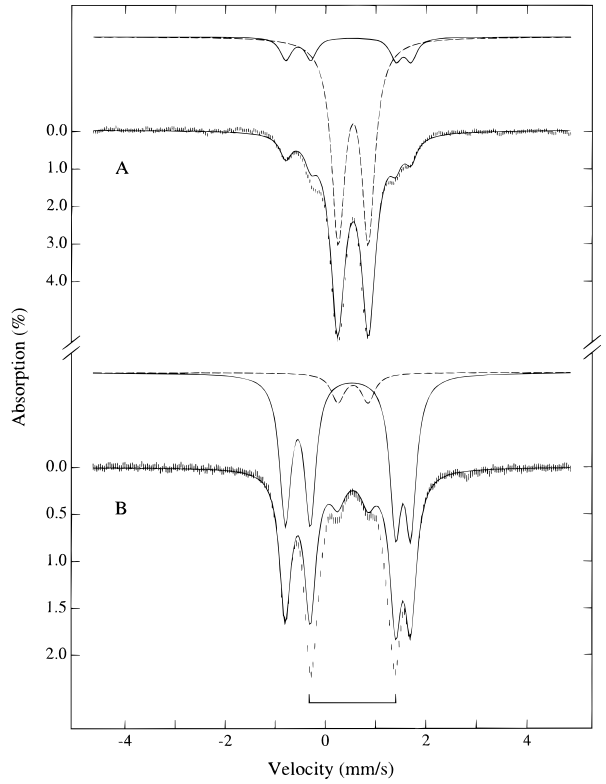

FIGURE 3: Mössbauer spectra at 4.2 K of R2-F208Y reacted as described in the legend to Figure 1 (A) in the absence of ascorbate and (B) in the presence of 106 mM sodium ascorbate. The solid and dashed lines plotted above each experimental spectrum are the reference spectra of the μ-oxo-diiron(III) cluster and the diiron(III)−catecholate, respectively. For spectrum A, their intensities correspond to 16% [μ-oxo-diiron(III) cluster] and 82% [diiron(III)−catecholate] of the total iron absorption, and for spectrum B, 76% [μ-oxo-diiron(III) cluster] and 10% [diiron(III)−catecholate] of the total iron absorption. The solid line plotted over each spectrum is the sum of the reference spectra at the indicated percentages. For each Mössbauer sample, five identical 500 μL samples of [R2-F208Y] = 0.10 mM were pooled and concentrated to 500 μL, as described in Materials and Methods. Spectral parameters are given in Materials and Methods.

μ-oxo bridge, as was seen crystallographically for the diiron(III)−catecholate (*22*); and (3) in experiments with increasing concentration of ascorbate, the intensity of this Mössbauer doublet was found to decrease in parallel with the intensity of the optical absorption feature at 675 nm (vide infra). In addition to the central doublet of the diiron(III)−catecholate, the Mössbauer spectrum has weaker features (16% ± 4%, solid line plotted above the data) that can be analyzed with parameters that are virtually identical with those of the wild-type μ-oxo-diiron(III) cluster (Table 1). The 0.24 ± 0.06 equiv of μ-oxo-diiron(III) cluster reflected by these features correlates well with the 0.25 ± 0.04 equiv of Y122 radical detected by EPR. Subtraction of the sum of the diiron(III)−catecholate and μ-oxo-diiron(III) cluster spectra (solid line plotted over the experimental spectrum) from the experimental spectrum reveals the presence of a third, minor component, which we have not yet definitively assigned.[6]

Table 1: Mössbauer Parameters of the Diiron(III)−Catecholate and the μ-Oxo-diiron(III) Cluster in R2-F208Y[a]

	diiron(III) product	Fe site	δ (mm/s)	ΔE_Q (mm/s)	line width, Γ (mm/s)
R2-F208Y	diiron(III)−catecholate	1	0.54 ± 0.02	0.60 ± 0.03	0.32
		2			
R2-F208Y	μ-oxo-diiron(III) cluster	1	0.45 ± 0.02	2.50 ± 0.04	0.27
		2	0.55 ± 0.04	1.70 ± 0.06	0.27
R2-wt[b]	μ-oxo-diiron(III) cluster	1	0.45 ± 0.02	2.41 ± 0.04	0.27
		2	0.54 ± 0.02	1.64 ± 0.04	0.27

[a] The parameters for the μ-oxo-diiron(III) cluster in wild-type R2 are also shown for comparison. [b] Data taken from ref *26*.

As noted above, the formation of ~0.25 equiv [out of 1.5 equiv total diiron(III) product] of the wild-type reaction products [μ-oxo-diiron(III) cluster and Y122 radical] suggests that the reaction partitions as depicted in Scheme 2. We reasoned that the partition ratio might be shifted to favor Y122 radical production (which involves injection of an exogenous electron from solution; step B of Scheme 2) over Y208 hydroxylation by carrying out the reaction in the presence of a facile one-electron donor, such as ascorbate. Indeed, with increasing concentration of ascorbate, the 675 nm band of the diiron(III)−catecholate develops to a lesser extent and the 365 nm feature of the μ-oxo-diiron(III) cluster to a greater extent upon reaction of the Fe^{2+}−R2-F208Y complex with O_2 (Figure 4). At the highest concentration of ascorbate, under which conditions the 675 nm feature of the diiron(III)−catecholate is nearly absent, the sharp 410 nm feature of the tyrosyl radical (Figure 1, thinner solid line) is comparable in intensity to that produced in the wild-type protein (Figure 1, dashed line) in the absence of ascorbate. Spin quantitation by EPR of this R2-F208Y sample (Figure 2, spectrum B) gave 1.0 ± 0.1 equiv of tyrosyl radical, comparable to the 1.2 ± 0.1 equiv formed in the wild-type protein (Figure 2, spectrum C). Similarly, the Mössbauer spectrum (Figure 3, spectrum B) indicates that 1.14 ± 0.1 equiv of the μ-oxo-diiron(III) cluster (solid line above the data) and only 0.15 ± 0.06 equiv of the diiron(III)−catecholate (dashed line above the data) are produced in the

[6] The unassigned features (marked by the bracket in Figure 3B) are observed both in the absence and in the presence of ascorbate, but they increase in intensity with increasing ascorbate concentration in parallel with the features of the μ-oxo-diiron(III) cluster. It is possible that they arise from a cluster in which the unmodified Y208 (lower pathway of Scheme 2) ligates Fe_A in monodentate fashion [i.e., a diiron(III)−tyrosinate].

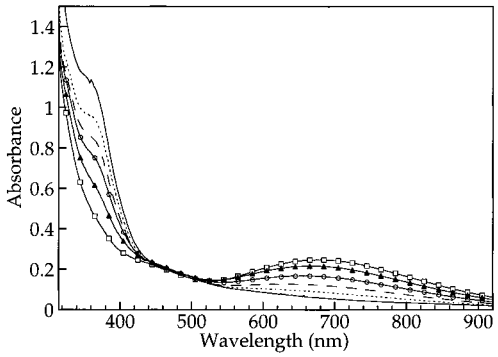

FIGURE 4: Effect of increasing ascorbate concentration on the diiron(III) products of the reaction of Fe^{2+}−R2-F208Y with excess O_2, as monitored by UV−visible absorption spectroscopy. For these samples, tyrosyl radical was allowed to decay for 1 h prior to acquisition of the spectra in order to highlight the features of the two different diiron(III) products. The sodium ascorbate concentrations were (□) 0 mM, (▲) 1.6 mM, (○) 6.6 mM, (− − −) 13 mM, (···) 26 mM, and (—) 106 mM. Details of sample preparation are given in Materials and Methods.

O_2 reaction with 106 mM ascorbate, compared to 0.24 ± 0.06 and 1.23 ± 0.06 equiv, respectively, in the absence of ascorbate (Figure 3A).[6] Thus, ascorbate *can* shift the partition ratio (by nearly 40-fold at 106 mM) to favor the normal products [tyrosyl radical and μ-oxo-diiron(III) cluster] over the Y208-derived diiron(III)−catecholate, consistent with the original hypothesis that it might promote electron injection and render this step increasingly rapid relative to the competing unimolecular step that leads to Y208 hydroxylation (Scheme 2, step A). An alternative explanation is that, at these high concentrations, ascorbate may diffuse into the cluster site and act as an "inner-sphere" reductant to alter the reaction outcome.

Effect of Varying Ascorbate Concentration on Products of O_2 Reaction of R2-W48F/F208Y. To distinguish between these possibilities, we sought to assess whether a specific electron-transfer pathway mediates the effect of ascorbate on the partition ratio (which would argue for electron injection over inner-sphere reduction). We have proposed for wild-type R2 that a hydrogen-bond network involving W48, D237, and H118 mediates the rapid electron injection that occurs during its O_2 reaction (*32*),[7] a hypothesis that is supported by our recent studies on the W48F site-directed mutant of R2.[8] To assess whether this pathway might mediate electron injection from ascorbate in the R2-F208Y reaction, we introduced the W48F mutation into R2-F208Y. As in the single mutant, reaction of the Fe^{2+} complex of R2-W48F/F208Y with O_2 in the absence of ascorbate results in the development of the 675 nm absorption characteristic of the diiron(III)−catecholate (Figure 5, solid line). Notably, the 410 nm feature characteristic of the tyrosyl radical does not develop, in contrast to the reaction of the F208Y single mutant. The Mössbauer spectrum of the product (Figure 6, spectrum A) indicates that 1.41 ± 0.06 equiv of the diiron(III)−catecholate but only 0.06 ± 0.04 (near the limit of detection) of the μ-oxo-diiron(III) cluster are produced. Thus, the W48F mutation shifts the partition ratio almost completely to hydroxylation of Y208. Most significantly, the W48F mutation completely eliminates the effect of ascorbate on the partition ratio: even 128 mM ascorbate has *no significant effect* on the UV−visible (Figure 5, dotted line) or Mössbauer spectra (Figure 6, spectrum B) of the products of the R2-W48F/F208Y O_2 reaction.

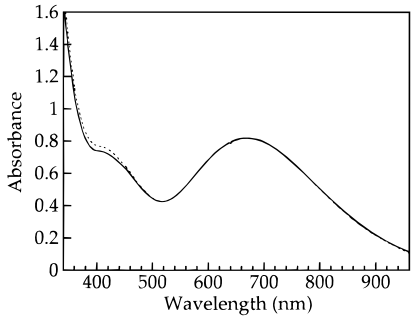

FIGURE 5: UV−visible light absorption spectra produced upon reaction at 5 ± 3 °C of Fe^{2+}−R2-W48F/F208Y (0.10 mM protein, Fe^{2+}/R2 = 3) with excess O_2 (~650 μM) in the absence of reductant (—) or in the presence of 128 mM sodium ascobate (···). Details of sample preparation are given in Materials and Methods.

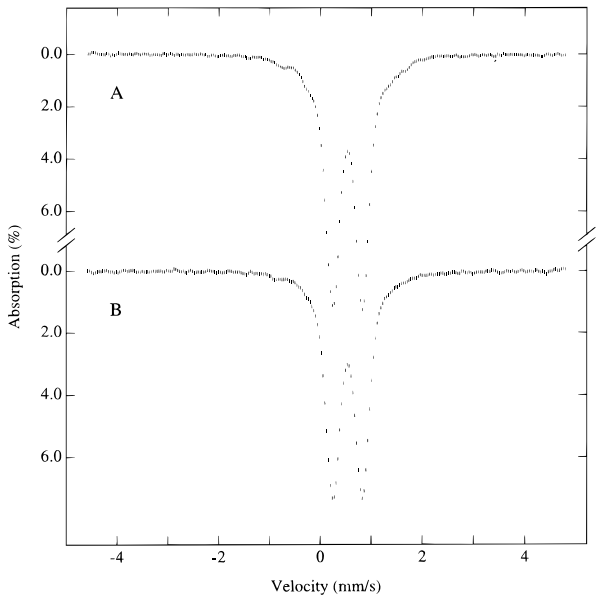

FIGURE 6: Mössbauer spectra of R2-W48F/F208Y reacted as described in the legend to Figure 5 (A) in the absence of ascorbate and (B) in the presence of 128 mM sodium ascorbate. For each Mössbauer sample, five identical 500 μL samples of [R2-W48F/F208Y] = 0.10 mM were pooled and concentrated to 500 μL, as described in Materials and Methods.

The most obvious interpretation of these data is that W48F is [as we previously proposed (*32*)] an essential constituent of a specific pathway for electron transfer between the R2 surface and the diiron cluster and that this pathway mediates electron injection by ascorbate, thereby allowing the partition ratio to be shifted to favor Y122 one-electron oxidation over Y208 hydroxylation by increasing concentration of the reductant. In the simplest case, the W48F mutation abolishes electron injection from ascorbate by disrupting this pathway. Alternatively, the electron transfer step may be "conformationally gated," and the W48F mutation may alter important local conformational dynamics. In either case, the conclusion that there is a specific pathway for electron transfer into the

[7] We note that Nordlund and co-workers first proposed, on the basis of the three-dimensional structure of R2, that this network is a specific pathway for electron transfer from the R1 subunit of RNR to the tyrosyl radical in R2 during the enzyme's catalytic mechanism.

[8] S. Chen, S. E. Parkin, C. Krebs, B. A. Ley, D. E. Edmondson, B. H. Huynh, and J. M. Bollinger, Jr., manuscript in preparation.

R2 cofactor would be valid, given that ascorbate bathing the surface of R2-W48F/F208Y is ineffective for electron injection. A third possibility is that ascorbate accesses the cluster site directly in R2-F208Y but is precluded from cluster access in R2-W48F/F208Y by a structural or dynamical perturbation resulting from the nonisosteric W48F mutation. We consider this possibility to be unlikely, as we have seen that the W48F mutation *does not* significantly perturb the rate constant of the slow protein conformational change that is required for formation of the O_2-reactive Fe^{2+}−R2 complex from apo-R2 and Fe^{2+} (*27*) (e.g., in comparing wild-type R2 with R2-W48F).[8] This observation suggests that access to the active site by Fe^{2+} is not noticeably altered by the W48F mutation. We hope ultimately to distinguish among the above possibilities by direct measurement of the individual rate constants of the constitutent steps of Scheme 2 in ongoing freeze−quench EPR and Mössbauer experiments.

The present data are consistent with the hypothesis that W48F is part of a specific electron-transfer pathway into the R2 cluster site of R2-F208Y. This conclusion lends credence to the hypothesis that the pathway involving W48 is operant in electron injection in the wild-type R2 reaction (*32*). Facilitating this process may be a (perhaps the) primary means by which the R2 protein directs the mechanism and outcome of its O_2 reaction, as this step ensures that no intermediate containing two oxidizing equivalents [such as the (formally) diiron(IV) compound Q that is thought to be the hydroxylating intermediate in the catalytic cycle of methane monooxygenase (*28*−*30*)] will accumulate. Were such a species to form in the R2 active site, alternative reactions such as self-hydroxylation might compete with the desired one-electron oxidation of Y122.

REFERENCES

1. Nordlund, P., and Eklund, H. (1995) *Curr. Opin. Struct. Biol. 5*, 758−766.
2. Wallar, B. J., and Lipscomb, J. D. (1996) *Chem. Rev. 96*, 2625−2657.
3. Fox, B. G., Shanklin, J., Somerville, C., and Münck, E. (1993) *Proc. Natl. Acad. Sci. U.S.A. 90*, 2486−2490.
4. Fox, B. G., Shanklin, J., Ai, J., Loehr, T. M., and Sanders-Loehr, J. (1994) *Biochemistry 33*, 12776−12786.
5. Lindqvist, Y., Huang, W., Schneider, G., and Shanklin, J. (1996) *EMBO J. 15*, 4081−4092.
6. Woodland, M. P., Patil, D. S., Cammack, R., and Dalton, H. (1986) *Biochim. Biophys. Acta 873*, 237−242.
7. Fox, B. G., Surerus, K. K., Münck, E., and Lipscomb, J. B. (1988) *J. Biol. Chem. 263*, 10553−10556.
8. Fox, B. G., Froland, W. A., Dege, J. E., and Lipscomb, J. D. (1989) *J. Biol. Chem. 264*, 10023−10033.
9. Rosenzweig, A. C., Nordlund, P., Takahara, P. M., Frederick, C. A., and Lippard, S. J. (1995) *Chem. Biol. 2*, 409−418.
10. Elango, N., Radhakrishnan, R., Froland, W. A., Wallar, B. J., Earhart, C. A., Lipscomb, J. D., and Ohlendorf, D. H. (1997) *Protein Sci. 6*, 556−568.
11. Pikus, J. D., Studts, J. M., Achim, C., Kauffmann, K. E., Munck, E., Steffan, R. J., McClay, K., and Fox, B. G. (1996) *Biochemistry 35*, 9106−9119.
12. Shanklin, J., Achim, C., Schmidt, H., Fox, B. G., and Munck, E. (1997) *Proc. Natl. Acad. Sci. U.S.A. 94*, 2981−2986.
13. Atkin, C. L., Thelander, L., Reichard, P., and Lang, G. (1973) *J. Biol. Chem. 248*, 7464−7472.
14. Sjöberg, B.-M., Reichard, P., Gräslund, A., and Ehrenberg, A. (1977) *J. Biol. Chem. 252*, 536−541.
15. Nagai, J., and Bloch, K. (1966) *J. Biol. Chem. 241*, 1925−1927.
16. Dalton, H. (1980) *Adv. Appl. Microbiol. 26*, 71−87.
17. Nordlund, P., and Eklund, H. (1993) *J. Mol. Biol. 232*, 123−164.
18. Logan, D. T., Su, X.-D., Åberg, A., Regnström, K., Hajdu, J., Eklund, H., and Nordlund, P. (1996) *Structure 4*, 1053−1064.
19. Salowe, S. P., and Stubbe, J. (1986) *J. Bacteriol. 165*, 363−366.
20. Sjöberg, B.-M., Hahne, S., Karlsson, M., Jörnvall, H., Göransson, M., and Uhlin, B. E. (1986) *J. Biol. Chem. 261*, 5658−5662.
21. Sjöberg, B.-M., Karlsson, M., and Jörnvall, H. (1987) *J. Biol. Chem. 262*, 9736−9743.
22. Åberg, A., Ormö, M., Nordlund, P., and Sjöberg, B.-M. (1993) *Biochemistry 32*, 9845−9850.
23. Ormö, M., deMaré, F., Regnström, K., Åberg, A., Sahlin, M., Ling, J., Loehr, T. M., Sanders-Loehr, J., and Sjöberg, B.-M. (1992) *J. Biol. Chem. 267*, 8711−8714.
24. Bollinger, J. M., Jr., Edmondson, D. E., Huynh, B. H., Filley, J., Norton, J. R., and Stubbe, J. (1991) *Science 253*, 292−298.
25. Bollinger, J. M., Jr., Stubbe, J., Huynh, B. H., and Edmondson, D. E. (1991) *J. Am. Chem. Soc. 113*, 6289−6291.
26. Bollinger, J. M., Jr., Tong, W. H., Ravi, N., Huynh, B. H., Edmondson, D. E., and Stubbe, J. (1994) *J. Am. Chem. Soc. 116*, 8015−8023.
27. Tong, W. H., Chen, S., Lloyd, S. G., Edmondson, D. E., Huynh, B. H., and Stubbe, J. (1996) *J. Am. Chem. Soc. 118*, 2107−2108.
28. Lee, S.-K., Fox, B. G., Froland, W. A., Lipscomb, J. D., and Münck, E. (1993) *J. Am. Chem. Soc. 115*, 6450−6451.
29. Lee, S.-K., Nesheim, J. C., and Lipscomb, J. D. (1993) *J. Biol. Chem. 268*, 21569−21577.
30. Liu, K. E., Wang, D., Huynh, B. H., Edmondson, D. E., Salifoglou, A., and Lippard, S. J. (1994) *J. Am. Chem. Soc. 116*, 7465−7466.
31. Ormö, M., Regnström, K., Wang, Z., Que, L., Jr., Sahlin, M., and Sjöberg, B.-M. (1995) *J. Biol. Chem. 270*, 6570−6576.
32. Bollinger, J. M., Jr., Ravi, N., Tong, W. H., Huynh, B. H., Edmondson, D. E., and Stubbe, J. (1994) *J. Am. Chem. Soc. 116*, 8024−8032.
33. Rova, U., Goodztzova, K., Ingemarson, R., Behravan, G., Gräslund, A., and Thelander, L. (1995) *Biochemistry 34*, 4267−4275.
34. Ekberg, M., Sahlin, M., Eriksson, M., and Sjöberg, B.-M. (1996) *J. Biol. Chem. 271*, 20655−20659.
35. Gill, S. C., and von Hippel, P. H. (1989) *Anal. Biochem. 182*, 319−326.
36. Thelander, L. (1973) *J. Biol. Chem. 248*, 4591−4601.
37. Malmström, B., Reinhammar, B., and Vänngård, T. (1970) *Biochim. Biophys. Acta 205*, 48.
38. Aasa, R., and Vänngård, T. (1975) *J. Magn. Reson. 19*, 308−315.
39. Ravi, N., Bollinger, J. M., Jr., Huynh, B. H., Edmondson, D. E., and Stubbe, J. (1994) *J. Am. Chem. Soc. 116*, 8007−8014.
40. Bollinger, J. M., Jr. (1993) On the Chemical Mechanism of Assembly of the Tyrosyl Radical-Dinuclear Iron Cluster Cofactor of *E. coli* Ribonucleotide Reductase, Ph.D. Thesis, Massachusetts Institute of Technology, Cambridge, MA.
41. Bender, C. J., Sahlin, M., Babcock, G. T., Barry, B. A., Chandrashekar, T. K., Salowe, S. P., Stubbe, J., Lindström, B., Petersson, L., Ehrenberg, A., and Sjöberg, B.-M. (1989) *J. Am. Chem. Soc. 111*, 8076−8083.
42. Barry, B. A., el-Deeb, M. K., Sandusky, P. O., and Babcock, G. T. (1990) *J. Biol. Chem. 265*, 20139−20143.
43. Sahlin, M., Petersson, L., Gräslund, A., Ehrenberg, A., Sjöberg, B.-M., and Thelander, L. (1987) *Biochemistry 26*, 5541−5548.
44. Hirsh, D. J., Beck, W. F., Lynch, J. B., Que, L., Jr., and Brudvig, G. W. (1992) *J. Am. Chem. Soc. 114*, 7475−7481.
45. Salowe, S. P. (1987) Ph.D. Thesis, University of Wisconsin, Madison, WI.

BI9723717